Published in final edited form as:
*Chem Res Toxicol*. 2008 October ; 21(10): 1939–1948. doi:10.1021/tx8001274.

# *Angelica sinensis* and its Alkylphthalides Induce the Detoxification enzyme NAD(P)H: Quinone OxidoReductase 1 by Alkylating KEAP1

**Birgit M. Dietz**[1,*], **Dongting Liu**[1], **Ghenet K. Hagos**, **Ping Yao**, **Andreas Schinkovitz**, **Samuel M. Pro**[†], **Shixin Deng**, **Norman R. Farnsworth**, **Guido F. Pauli**, **Richard B. van Breemen**, and **Judy L. Bolton**

*Department of Medicinal Chemistry and Pharmacognosy, UIC/NIH Center for Botanical Dietary Supplements Research, University of Illinois at Chicago, 833 S. Wood Street, M/C 781, Chicago, IL 60612−7231, USA*

†*Institute for Tuberculosis Research, University of Illinois at Chicago, 833 S. Wood Street, M/C 781, Chicago, IL 60612−7231, USA*

## Abstract

The roots of *Angelica sinensis* (Oliv.), Diels (Dang Gui; Apiaceae) have a long history in traditional Chinese medicine as a remedy for women's disorders, and are often called “lady's ginseng”. Currently, extracts of *A. sinensis* are commonly included in numerous dietary supplements used for women's health and as anti-aging products. In the present study, we examined the potential chemopreventive activity of *A. sinensis* extracts by measuring the relative ability to induce the detoxification enzyme, NAD(P)H:quinone oxidoreductase 1 (NQO1). The lipophilic partitions showed strong NQO1 induction with concentrations to double the enzyme activity (CD) of 5.5 ± 0.7 μg/mL (petroleum ether) and 3.9 ± 0.5 μg/mL (chloroform). Fractionation led to the isolation of phenolic esters and alkylphthalides, especially *Z*-ligustilide, the main lipophilic compound, which showed strong NQO1 inducing properties (CD = 6.9 ± 1.9 μM). Transcription of many detoxifying enzymes is regulated through the antioxidant response element (ARE) and its transcription factor Nrf2, which is repressed under basal conditions by Keap1. However, exposure to electrophilic inducers that alkylate Keap1 results in a higher concentrations of free Nrf2 and ARE activation. The ARE reporter activity was therefore analyzed in HepG2-ARE-C8 cells after incubation with lipophilic extracts of *A. sinensis* or ligustilide for 24 h. Under these conditions, both the extract and ligustilide increased ARE-luciferase reporter activity in a dose-dependent manner. Incubation of ligustilide with GSH and subsequent LC-MS-MS analysis revealed that ligustilide as well as oxidized ligustilide species covalently modified GSH. In addition, using MALDI-TOF mass spectrometry and LC-MS-MS, it was demonstrated that the lipophilic extracts, ligustilide, and monooxygenated ligustilide alkylated important cysteine residues in human Keap1 protein, thus activating Nrf2 and transcription of ARE regulated genes. These observations suggest that *A. sinensis* dietary supplements standardized to ligustilide have potential as chemopreventive agents through induction of detoxification enzymes.

### Keywords

*Angelica sinensis*; alkylphthalides; cancer chemoprevention; Dang Gui; detoxification enzymes; Keap1; ligustilide; NAD(P)H: quinone reductase 1; Nrf2; oxidative stress

*To whom correspondence should be addressed. Fax: (312) 996−7107, Tel.: (312) 996−2358, Email: birgitd@uic.edu.
[1]These authors contributed equally.

## Introduction

The dried roots of *Angelica sinensis* (Oliv.) Diels, Apiaceae (Dong Quai or Dang Gui) have been used for centuries as “women's tonic” especially for alleviating menstrual disorders or menopausal symptoms in Asia (1-7). Recently, pharmacological research has focused on elucidating the antioxidative, cancer preventive, and overall oxidative stress reducing properties of *A. sinensis* (3,8). For example, it has been reported that lipophilic extracts as well as *n*-butylidenephthalide isolated from the chloroform extract exert antiproliferative effects on tumor cells *in vitro* and *in vivo* (9-12). In addition, recent data revealed that *Z*-ligustilide, the major lipophilic constituent in *A. sinensis*, reduces oxidative stress in brain tissue possibly through increasing antioxidative enzymes, such as glutathione peroxidase and superoxide dismutase, and reducing apoptotic markers (6,13). It has also been demonstrated that *A. sinensis* can protect cardiomyocytes against oxidant injury by increasing cellular GSH, suggesting a cardioprotective effect (14). These activities indicate that *A. sinensis* can reduce cellular oxidative stress, which can be useful in the prevention of cancer as well as neuro- and cardiovascular diseases. However, the mechanism by which *A. sinensis* exerts chemopreventive activity has not been elucidated.

To survive under a variety of environmental or intracellular stresses, eukaryotic cells have developed cellular defensive systems to protect themselves from oxidative or electrophilic challenges (15). The removal of reactive electrophiles causing oxidative stress or initiating carcinogenic processes can be accomplished by detoxification enzymes which eliminate electrophiles by reduction or conjugation to make them less reactive or facilitate their excretion (16). As a result, the induction of detoxification enzymes, including NAD(P)H: quinone oxidoreductase 1 (NQO1) and glutathione-S-transferase (GST), by natural agents is important for cancer prevention and for cytoprotection in general (17,18). Many of these detoxifying enzymes are coordinately regulated through the antioxidant response element (ARE), which is mainly controlled by two proteins, Keap1 and Nrf2 (19,20). Keap1 is a cysteine rich, cytosolic inhibitor of Nrf2, which is a transcriptional activator of ARE regulated genes (21). One hypothesis of enzyme induction suggests that electrophilic species can alkylate cysteine residues in Keap1 (22) resulting in higher levels of Nrf2 in the nucleus, where it binds to the 5’-upstream regulatory ARE regions of detoxification genes and accelerates their transcription (Scheme 1) (17,20,23). For example, sulforaphane isolated from broccoli (*Brassica* spp.) is an example of a potent inducer of Nrf2-ARE regulated detoxification enzymes including NQO1 that has demonstrated anticarcinogenic properties as well as cardio- and neurovascular protection *in vivo* (24-28). Furthermore, various natural and synthetic compounds with an α,β-unsaturated ketone functionality have been shown to alkylate cysteines in Keap1 resulting in NQO1 induction (29-32).

The characteristic constituents of *A. sinensis* are various alkylphthalides with *Z*-ligustilide as the major representative of this class of Apiaceaous phytoconstituents (Figure 1) (33). Ligustilide accounts for 45−60% of the volatile oil and occurs at a total concentration of ~12 mg/g root (34-36). Dihydrophthalides, such as ligustilide, have an α,β,γ,δ -unsaturated lactone moiety with a cross-conjugated alkene system and, therefore, contain multiple Michael reactive sites (33). It has been shown that thiol nucleophiles react slowly with the 3,8-ene by 1,6-Michael addition (37).

Since the non-aromatic phthalides are known to be weak electrophiles and, therefore, have the potential to react with sulfhydryl groups, such as in Keap1, extracts of *A. sinensis* might induce detoxification enzymes and hence prevent cellular oxidative stress. On the basis of this information, the cytoprotective potential of *A. sinensis* and its underlying mechanism was analyzed in detail.

## Material and Methods

### Materials

All chemicals and reagents were obtained from Fisher Scientific (Hanover Park, IL) or Sigma-Aldrich (St. Louis, MO), unless stated otherwise. Cell culture media and supplements were obtained from Invitrogen (Carlsbad, CA). Trypsin was purchased from Pierce (Milwaukee, WI). Recombinant Keap1 protein was a generous gift from Dr. Aimee L. Eggler and Dr. Andrew D. Mesecar (University of Illinois at Chicago). Dried roots of *Angelica sinensis* (Oliv.) diels were purchased from Kiu Shun Trading Ltd. (Vancouver, Canada) in 2000, and identified using a series of comparative macroscopic, microscopic, TLC, HPLC, and PCR analysis with *A. sinensis* reference plant materials obtained from the National Institute for the Control of Pharmaceutical and Biological Products of China, Beijing, People's Republic of China (Lot # 927−200110) (1).

### Extraction and isolation

The milled roots (8.0 kg) of *A. sinensis* were macerated in 20 L of methanol for 24 h and then percolated exhaustively with the same solvent (total 40 L). The chloroform, petroleum ether, *n*-BuOH, and water partitions were obtained as described by Deng et al. (1). The two active fractions, the chloroform and petroleum ether partition, were combined and then fractionated by flash column chromatography with subsequent vacuum liquid chromatography and semi-preparative HPLC. The detailed isolation steps and characterization of the tested compounds were described previously (1). The purity of the compounds was assessed by GC-MS and NMR. Freshly isolated ligustilide showed a purity (GC-MS) of 98.6%, which degraded in dry state over 24 h at room temperature to 58.1% (38). For all experiments except for these degradation studies, degradation of ligustilide **1** was avoided by storing it at −80 °C and in organic solution (hexane/EtOAC, 9:1). Because ligustilide and its alkylphthalides were enriched in the petroleum ether partition, the following experiments were performed with this partition, if not otherwise specified. According to GC-MS TIC experiments the petroleum ether partition contained 5−8% ligustilide.

### Cell culture conditions

Hepa1c1c7 murine hepatoma cells were supplied by Dr. J. P. Whitlock, Jr. (Stanford University, Stanford, CA). Cells were maintained in α-minimum essential medium (MEME) supplemented with 1% penicillin-streptomycin, 10% fetal bovine serum (Atlanta Biologicals, Atlanta, GA), and incubated in 5% $CO_2$ at 37 °C. HepG2 cells stably transfected with ARE luciferase reporter (HepG2-ARE-C8) were kindly provided by Dr. A.N. Tony Kong (Rutgers University, Piscataway, NJ). Cells were grown in modified F-12 medium supplemented with 10% fetal bovine serum, 1.7 g/L sodium bicarbonate, 100 units/mL penicillin, 100 μg/mL streptomycin, essential amino acids, and insulin.

### DPPH assay

Reaction mixtures containing test samples (5 μL dissolved in DMSO or water) and 95 μL of a 200 μM 1,1-diphenyl-2-picrylhydrazyl (DPPH) ethanolic solution were incubated at 37 °C for 20 min in 96-well microtiter plates (39). Absorbance of the free radical DPPH was measured at 515 nm with an ELISA reader (Power Wave 200 Microplate Scanning Spectrophotometer, Bio-Tek Instrument, Winooski, VT), and the percent inhibition was determined by comparison with DMSO treated control groups. Each pure compound was screened at a concentration of 100 μM and the *A. sinensis* extracts at 100 μg/mL. Results represent the average ± SD of three determinations.

### *In vitro* NQO1 assay

Induction of NQO1 activity was assessed using Hepa-1c1c7 murine hepatoma cells as described previously with minor modifications (40,41). Briefly, Hepa-lclc7 cells were seeded in 96-well plates at a density of $1.25 \times 10^4$ cells/mL in 190 μL media. This cell concentration ensured that the cells reached 70−80% confluency until the end of the incubation period. After 24 h incubation, test samples were added to each well and the cells incubated for an additional 48 h. These incubation times have previously been shown to give the highest NQO1 induction results (40,41). The medium was decanted and the cells incubated at 37 °C for 10 min with 50 μL of 0.8% digitonin and 2 mM EDTA solution (pH 7.8). Next, the plates were agitated on an orbital shaker (100 rpm) for 10 min at room temperature, and then 200 μL of reaction mixture (bovine serum albumin, 3-(4,5-dimethylthiazo-2-yl)-2,5-diphenyltetrazolium bromide (MTT), 25 mM Tris-HCl, 0.01% Tween 20, 5 μM FAD, 1 mM glucose-6-phosphate, 30 μM NADP, glucose-6-phosphate dehydrogenase 2 units/mL, and 50 μM menadione) were added to each well. After 5 min, the plates were scanned at 595 nm. The specific activity of NQO1 was determined by measuring NADPH-dependent menadione-mediated reduction of MTT to form blue formazan. The resulting enzyme activity was divided by the protein concentration, which was determined by crystal violet staining on a separate plate at the same time. Induction of NQO1 activity was calculated by comparing the NQO1 specific activity of sample treated cells with that of solvent-treated cells. CD values represent the concentration required to double NQO1 induction. The chemopreventive index (CI) was then calculated, which is an indexing value generated by dividing the $IC_{50}$ by the CD value for a particular compound or extract ($IC_{50}$/CD) (29).

### Cytotoxicity assay

Cells were plated and treated as described for the NQO1 assay. After the cells were treated with test samples for 48 h, the medium was decanted, and 200 μL of 0.2% crystal violet (CV) solution in 2% ethanol was added. After 10 min, the plates were rinsed for 2 min with water and dried. The bound dye was solubilized by incubation at 37 °C for 1 h with 200 μL of 0.5% SDS in 50% ethanol. The absorption of crystal violet was measured at 595 nm, and the $IC_{50}$ values were determined.

### ARE-luciferase activity assay

HepG2-ARE-C8 cells were plated in six-well plates at a density of $1 \times 10^5$ cells/mL and incubated overnight (42). Cells were either stimulated with different concentrations of ligustilide or 4’-bromoflavone (BF, positive control, 664 nM) or with DMSO as negative control. After 24 h treatment, the luciferase activity was determined according to the protocol provided by the manufacturer (Promega, Madison, WI). Briefly, cells were washed with cold PBS and harvested in passive lysis buffer. After centrifugation, 20 μL of the supernatant was used for determining luciferase activity, which was measured by a luminometer (FLUOstar OPTIMA, BMG Labtechnologies, Offenburg, Germany). Luciferase activity was normalized to protein concentration using the BCA (bicinchoninic acid) protein assay (Pierce, Rockford, IL). The data were obtained from three separate experiments and expressed as fold-induction over control (treated cells/DMSO treated cells ± SD).

### LC-MS-MS analysis of GSH conjugates

The *A. sinensis* partition (100 μg/mL) and ligustilide (100 μM) were incubated individually with 1 mM GSH in a total volume of 200 μL of 25 mM Tris-HCl buffer (pH 8.0) for 1 h at room temperature. After incubation of the *A. sinensis* sample with GSH, the reaction product mixture was diluted 10-fold with water and analyzed using LC-MS-MS with a Thermo Electron (San Jose, CA) TSQuantum triple quadrupole mass spectrometer equipped with a Surveyor HPLC system and a Phenomenex (Torrance, CA) $C_{18}$ HPLC column (5 μM, 250 × 2.0 mm).

The solvent system consisted of a gradient with solvent A (5 mM ammonium acetate) and solvent B (methanol) at a flow rate of 200 μL/min. The 28 min gradient consisted of 5% B for 0−3 min, 5−80% B in 3−10 min, 80% B in 10−20 min, 80−90% B in 20−21 min, and 90% B in 21−28 min. Aliquots (20 μL) of each GSH reaction mixture were analyzed using LC-MS-MS with negative ion electrospray. Collision-induced dissociation (CID) and MS-MS scanning for precursors of the GSH fragment ion *m/z* 272 were used for the selective detection of GSH conjugates. Structural information for each conjugate was obtained using CID with product ion scanning. Accurate mass measurements of GSH conjugates were performed in positive ion mode electrospray using a Thermo Electron linear ion trap Fourier-transform ion cyclotron resonance (FT-ICR) mass spectrometer.

## Alkylation of Keap1

The *A. sinensis* partition (100 μg/mL) and ligustilide (100 μM) were incubated individually with 5 μM Keap1 in a total volume of 200 μL of 25 mM Tris-HCl buffer (pH 8.0) for 1 h at room temperature. As in our previous studies (43), the reducing agent Tris[2-carboxyethyl] phosphine hydrochloride (200 μM) was used to prevent the formation of any disulfide bonds within Keap1. The MALDI TOF mass spectrometer experiments were performed according to Liu et al. (43). Briefly, the matrix solution (1.0 μL) consisting of 10 mg/mL 3,5-methoxy-4-hydroxycinnamic acid in acetonitrile/water/trifluoroacetic acid (50:49.9:0.1; v/v/v) was mixed with 1.0 μL of the Keap1 incubation solution. This mixture (1.0 μL) was analyzed using positive ion MALDI-TOF mass spectrometry over the range of *m/z* 50,000−90,000 using an Applied Biosystems (Foster City, CA) Voyager DE-Pro instrument operated in linear mode.

## LC-MS-MS analysis of tryptic digested peptides

Ligustilide (100 μM) was incubated with 5 μM Keap1 in a total volume of 200 μL of 25 mM Tris-HCl buffer (pH 8.0) for 1 h at room temperature. Subsequently, the sample was quenched with excess of DTT (0.5 mM ). To block the remaining free cysteine residues, the mixture was treated with 1.5 mM iodoacetamide in DTT, allowed to react for 30 min, and treated with a final DTT addition (1 mM). Each Keap1 sample (modified or unmodified) was incubated with 6 μg/mL trypsin in Tris-HCl buffer (pH 8.0) at 37 °C for 3 h. Adjusting the pH to 3.5 using 10% trifluoroacetic acid solution stopped the digestion. A total of 10 μL of each sample was analyzed using a reversed phase LC-MS-MS system consisting of the linear ion trap FT-ICR mass spectrometer equipped with a Michrom Multi-Dimensional HPLC system and a Vydac (Hesperia, CA) $C_{18}$ reversed phase HPLC column (5 μm, 2.1 × 150 mm, 300 Å). The solvent system consisted of a gradient from solvent A (water/acetonitrile/formic acid; 95:4.9:0.1, v/v/v) to solvent B (water/acetonitrile/formic acid; 4.9:95:0.1, v/v/v) at a flow rate of 150 μL/min. The 60 min gradient consisted of 100% A for 0−5 min, 0−40% B from 5−40 min, 40−80% B from 40−50 min, and 80−100% B from 50−60 min. The column was maintained at 40 °C, and the sample compartment was set to 4 °C. Positive ion MS/MS spectra were acquired using data-dependent scanning with one MS scan followed by four MS/MS scans; the mass spectra were obtained over the range of *m/z* 400−2,000 for each analysis. Ions subjected to MS/MS were excluded from repeated analysis for 30 sec. The collision energy was set to 35%. The LC-MS-MS data were processed using BioWorks™ 3.1 (Thermo Electron). The alkylation sites were identified based on the tandem mass spectra of the peptides following a database search using TurboSEQUEST (Thermo Electron, Waltham, MA).

## Statistics

One-way ANOVA with Dunnett's post test was performed using GraphPad Prism version 4.00 for Windows (GraphPad Software, San Diego, CA, www.graphpad.com). In all cases, a $P$ value $< 0.05$ was considered significant. Experimental values are expressed as average ± SD.

## Results

### Antioxidative activity

Free radical scavenging is commonly regarded as one mechanism reducing cellular oxidative stress, as it protects lipids, proteins, and DNA against oxidative damage (44). The antioxidant activities of *A. sinensis* partitions and the isolated compounds were measured according to their relative ability to scavenge DPPH free radicals. Only the chloroform partition showed weak antioxidative activity with 60% free radical scavenging at a concentration of 100 μg/mL (Table 1). The chloroform partition contains various aromatic acids (1), such as the ferulic acid derivative, *p*-hydroxyphenethyl-trans-ferulate **7** (Figure 1), which showed moderate radical scavenging activity. However, the weak radical scavenging activity of *A. sinensis* extracts unlikely contributes to its overall chemopreventive effect.

### NQO1 activity

NQO1 catalyzes the detoxification of cytotoxic quinones such as menadione (45). For this reason, NQO1 helps protect cellular membranes, proteins, and DNA against oxidative damage. The measurement of NQO1 inducing properties in Hepa1c1c7 cells has been used extensively to assess the potential anticarcinogenic activity of natural products (46). The *A. sinensis* extracts, the phthalides, and other isolated compounds were tested for their NQO1 inducing activity (Table 1). Compounds or extracts were deemed to be active if their CD values (concentration to double NQO1 activity) were lower than 20 μM or 20 μg/mL (47). Partitioning of a methanol extract of *A. sinensis* revealed that the lipophilic partitions (petroleum ether, chloroform) showed favorable NQO1 inducing properties (Table 1). Further bioassay guided fractionation of the combined petroleum ether and chloroform partitions showed that some alkylphthtalides, especially the most abundant compound in the lipophilic fraction, ligustilide **1** (Figure 1), and also the phenolic esters **6** and **7**, had respectable NQO1 inducing activities (Table 1). Cell viability was determined to correct the observed NQO1 activity for cytotoxicity. The partitions and pure compounds with the exception of the dimer, ansaspirolide **4**, had no effect on cell viability at the tested concentrations. The chemopreventive index (CI), which is calculated as the ratio of the $IC_{50}$ value divided by the CD value ($IC_{50}$/CD), of ligustilide was 10, which is slightly lower than the chemopreventive effect of the well-known cancer chemopreventive compound sulforaphane (CI: 26) (29). Due to its potent NQO1 inducing properties, favorable CI value of 19, and high content of ligustilide, the petroleum ether partition of *A. sinensis* was used in the following experiments unless otherwise stated.

In contrast to ligustilide, which is characterized by a cyclohexadiene ring, its aromatic analogue, *Z*-butylidenephthalide **2** (Figure 1), did not induce NQO1 activity. One oxidized form of ligustilide, senkyonolide I **3**, showed only weak NQO1 inducing properties (Table 1). The two phthalide dimers, ansaspirolide **4** and sinaspirolide **5** are biogenetically formed from **2** and ligustilide as precursors (1). Interestingly, while **5** did not show any NQO1 inducing activity, **4** demonstrated potent inducing properties, although its cytotoxic effects ($IC_{50}$ = 2.9 μM) resulted in a low CI of 3.

Ligustilide has been reported to be a volatile and unstable compound (34,48). Therefore, the NQO1 inducing activity of freshly isolated ligustilide (GC-MS purity 98.6%) was compared to the activity of degraded ligustilide (58.1%). Interestingly, the NQO1 inducing activity of freshly isolated ligustilide was comparable to degraded ligustilide (Table 1) suggesting that the degradation products of ligustilide contribute to the overall NQO1 inducing activity.

### Induction of ARE-mediated reporter activity by *A. sinensis* partition and ligustilide

The ARE regulates the induction of detoxification enzymes, such as NQO1. HepG2-ARE-C8 cells, generated from HepG2 cells stably transfected with the pARE-TI-luciferase construct

(49), were treated with various concentrations of *A. sinensis* partition or ligustilide, and the luciferase activity was determined (Figure 2). Both the partition and pure ligustilide induced ARE reporter luciferase activity in a dose-dependent manner.

### Reaction of GSH with electrophiles in the *A. sinensis* partition

In order to screen for electrophilic compounds that alkylate sulfhydryl nucleophiles, the *A. sinensis* partition was incubated with GSH for 1 h at room temperature. Negative ion electrospray mass spectrometry with CID and precursor ion scanning was used to identify the deprotonated molecules of GSH conjugates that fragmented to form ions of *m/z* 272, corresponding to deprotonated γ-glutamyl-dehydroalanylglycine as described by Dieckhaus et al. (50). The negative ion LC-MS-MS precursor ion scan (Figure 3A) identified two major GSH conjugates. The GSH conjugate eluting at 15.0 min formed a deprotonated molecule of *m/z* 496 suggesting that ligustilide in the extract covalently modified GSH. The peak eluting at 15.4 min formed a deprotonated molecule of *m/z* 544 which corresponds to the mass of ligustilide plus GSH and three oxygen atoms. The exact structure of the latter eluting GSH conjugate is under investigation. Triple oxidized ligustilide derivatives, senkyunolide R and S, were isolated from *Ligusticum chuanxiong*, a species which contains very similar constituents to *A. sinensis* (33,51). Therefore, it is very likely that these triple oxidized ligustilide species, which exhibit the necessary α,β,γ,δ-unsaturated lactone moiety, could also occur in *A. sinensis*.

### Reaction of GSH with ligustilide

GSH also reacted with isolated ligustilide to form the same conjugate of *m/z* 496 eluting at 15.0 min (Figure 3B). Not detected in the incubation of the *Angelica* partition with GSH, another major GSH conjugate in the ligustilide incubation was observed at *m/z* 512 with a retention time of 15.1 min. This conjugate had a molecular mass corresponding to a monooxygenated ligustilide with a mass of 206 reacting with one molecule of GSH. Isolated ligustilide is unstable compared to ligustilide present in an extract, which may explain why this conjugate was not observed in incubations with the partition and GSH. Additional evidence for the proposed ligustilide GSH conjugates was obtained by high-resolution accurate mass measurement using a linear ion trap FT ICR mass spectrometer. The two proposed ligustilide GSH conjugates formed protonated molecules of *m/z* 498.1911 and 514.1860 that corresponded to ligustilide-GSH and oxidized ligustilide-GSH conjugates, respectively (Table 2). In both cases, the experimentally determined mass differed from the theoretical mass for the proposed elemental composition by less than 2 ppm (parts per million) confirming the molecular formulae (Table 2).

### Alkylation of Keap1

Recently, we developed a mass spectrometry-based method to screen complex mixtures such as botanical extracts for potential cancer chemopreventive agents, based on alkylation of Keap1 (43). Electrophilic constituents in the *A. sinensis* partition alkylated Keap1 (Figure 4A) and increased its mass by approximately 2,000 u. Keap1 contains 27 cysteine residues and in previous investigations with other Michael acceptors, we observed up to 12 different alkylated cysteine sites in Keap1 (31). Similar results were achieved by incubation of Keap1 with ligustilide (Figure 4B). After incubation with ligustilide, the mass of Keap1 increased approximately 644 u, indicating that ligustilide and/or oxidized ligustilide species alkylated multiple cysteine residues in Keap1 (Figure 4B).

### Sites of modification in human Keap1 by ligustilide species

In order to identify the sites of alkylation, peptide mapping and sequencing of alkylated Keap1 was carried out using high performance linear ion trap FT ICR LC-MS-MS. This approach has

been used previously to determine the modification pattern of Keap1 after alkylation by ARE inducers containing a Michael addition moiety (31). Ligustilide was incubated with Keap1 at 37 °C for 1 h, and then alkylated Keap1 was digested using trypsin followed by peptide mapping and sequencing. The accurate masses of ligustilide (190.0988) and monooxygenated ligustilide (206.0938) (Table 2) were used in the BioWorks™ software to search for peptide alkylation. Both ligustilide species were found to modify Keap1 exclusively at cysteine residues (Table 3). Whereas ligustilide only alkylated C151, oxidized ligustilide alkylated four cysteine residues including C151, C273, C288, and C319 (Table 3). These results show that ligustilide and monooxygenated ligustilide covalently modify specific sulfhydryl groups in Keap1.

## Discussion

*A. sinensis* is widely used as a dietary supplement for women's health, especially for the relief of postmenopausal symptoms and as an “anti-aging product” (1). Extracts of *A. sinensis* are usually standardized to a specific amount of the alkylphthalide, ligustilide **1**, since it is the major compound in lipophilic extracts (36). Numerous pharmacological activities have been attributed to ligustilide, such as smooth muscle relaxation, sedative, and antimicrobial effects (37,52,53). Recent studies have demonstrated cytoprotective and antiproliferative effects of the lipophilic extracts, ligustilide, and other phthalides indicating preventive potential against cancer as well as cardiovascular and neurodegenerative diseases (6,9,10,13). In this study, we examined the chemopreventive potential of *A. sinensis* extracts as well as of isolated compounds, especially ligustilide, by analyzing their antioxidative and their detoxification enzyme inducing properties.

Scavenging of free radicals by antioxidative compounds presents one pathway to reduce oxidative stress (54). The relative abilities of the extracts and compounds to scavenge the stable radical DPPH were determined (Table 1). Only the chloroform partition containing various polyphenolic acid esters showed moderate antioxidative activity (Table 1). Among the isolated compounds tested, only the ferulic acid ester **7** exhibited moderate activity (Table 1). These results are in agreement with previous literature reports. Wu et al. described weak antioxidative activity for the aqueous extract of *A. sinensis* (55). The essential oil exhibited moderate antioxidative activity in three different antioxidative assays including the DPPH assay ($IC_{50}$ = 194.7 μg/mL) (56). The most active fractions were characterized by a high coniferyl ferulate concentration (DPPH assay; $IC_{50}$ = 15.2 μg/mL 92% coniferyl ferulate) (56). Compared to other botanicals with strong antioxidative activity, for example green tea, which showed an $IC_{50}$ in the DPPH assay of approximately 14 μg/mL (57), the radical scavenging effects of *A. sinensis* are weak and unlikely to contribute to the overall chemopreventive activity of *A. sinensis*.

The NQO1 inducing activities of *A. sinensis* partitions and its compounds were also investigated. NQO1 catalyzes two-electron reduction of quinones. This prevents the formation of unstable semiquinones and ROS, which are generated by cytochrome P450 reductase that catalyzes one-electron reduction of quinones (58). The unstable semiquinones undergo redox cycling in the presence of molecular oxygen generating ROS and causing oxidative stress potentially leading to cellular damage, mutagenesis, and/or carcinogenesis (59-61). NQO1 plays an important role in cancer prevention, but it is also essential for the risk reduction of other chronic diseases. For example, it has been demonstrated that NQO1 induction may have athero- and cardioprotective properties (62,63). However, it should be noted that in some cases NQO1 calalyzes the reduction of xenobiotics to toxic intermediates or metabolites (64). For example, mitomycin C is bioactivated in tumors with elevated NQO1 activity (65).

Our data indicated that lipophilic partitions rich in alkylphthalides showed potent NQO1 inducing properties (Table 1). The major alkylphthalide, ligustilide, demonstrated significant

inducing activity, which could be explained by the α,β,γ,δ -unsaturated lactone moiety with the cross-conjugated alkene system (Figure 1) reacting in a Michael fashion with nucleophiles (33,48). In contrast, **2** represents a classical alkylphthalide with an aromatic ring instead of the cross conjugated alkene system (Figure 1). Therefore, the 3,8 alkene group is less reactive and in accordance with the theory that the inducer capacity parallels the reactivity of the Michael acceptor group, **2** did not show NQO1 inducing properties at the concentrations tested (Table 1) (66). Similarly, in senkyonolide I **3** the 6,7 alkene group of ligustilide is converted to two hydroxyl groups, and the 3,8-ene group is less active compared to ligustilide resulting in moderate NQO1 inducing properties. Interestingly, the relative NQO1 activities of the two dimeric phthalides were distinct from each other. Only **4** showed potent NQO1 inducing activity, which was combined with high cytotoxicity, leading to a low CI value. In contrast to **5**, dimer **4** has the requisite conjugated unsaturation moiety, which might explain its NQO1 inducing properties.

Aromatic esters with α,β-unsaturated keto functional groups, such as cinnamic acid esters, have been shown to be potent NQO1 inducing compounds (67). The ferulic acid ester derivatives **6** and **7** showed high NQO1 inducing properties (Table 1). Compound **7** has been previously isolated from green onions, and its NQO1 inducing properties were found to be similar to the results reported here (CD: 6.6 μM) (68). Compounds **6** and **7**, which are mainly present in the chloroform partition, could contribute to the NQO1 inducing effects of the crude extract; however, the enhanced electrophilicity of ligustilide as well as its higher concentration implicates ligustilide as the major species responsible for NQO1 induction (36).

The transcription of several detoxification enzymes, including GST, epoxide hydrolase, heme oxygenase, thioredoxin reductase, and NQO1 among others, is mediated by the ARE (15). Both the *A. sinensis* extract and ligustilide induced ARE reporter activity in a dose-dependent fashion (Figure 2). The induction of ARE regulated detoxification enzymes can protect against various oxidant and electrophilic agents and hence prevent various diseases associated with oxidative stress (19).

Keap1 and Nrf2 are mainly involved in regulating the expression of detoxification enzymes and antioxidant proteins through the ARE (Scheme 1) (20,69). Under basal conditions, the transcription factor Nrf2 is repressed by Keap1 in the cytosol and unable to activate the ARE. One theory of detoxification enzyme induction states that upon introduction of inducing agents, which can oxidize or alkylate highly reactive cysteine residues in Keap1 (22), Nrf2 accumulates in the nucleus, where it binds to the ARE and accelerates the transcription of detoxification genes (20,23,70). Therefore, we examined whether the petroleum ether partition and ligustilide could modify sulfhydryl groups in GSH and in human Keap1 protein. LC-MS-MS analysis of GSH incubations with *A. sinensis* partition or ligustilide revealed that the lipophilic partition as well as ligustilide formed GSH conjugates (Figure 3). The expected product corresponding to the mass of ligustilide plus GSH was observed at *m/z* 496. In addition, another major GSH conjugate of *m/z* 512 was detected representing the reaction of a monooxygenated ligustilide species (mass: 206) with GSH (34). Ligustilide is an unstable compound, which quickly forms epoxidized (Figure 5) and other oxygenated dihydrophthalides (Figure 1, compound **3**) and butylidene species, such as compound **2**, as well as dimeric butylidene phthalides, for example compounds **4** and **5** (Figure 1) (1,33,34,48,71). Some of these compounds, such as **2**, **3**, **4**, and **5**, occur naturally in the plant, but can also be generated through degradation of purified ligustilide. Regarding the degradation of ligustilide to a monooxygenated ligustilide species (mass: 206), Lin et al. reported that ligustilide is oxidized to *Z*-6,7-epoxyligustilide (Figure 5) which hydrolyzes to senkyonolide I **3** (Figure 1) (34). In addition, it has been suggested that oxidation to 3,8-epoxyligustilide and subsequent cleavage to phthalic anhydride represents one major degradation pathway for ligustilide (38). Therefore, these electrophilic oxidation

products may covalently modify GSH or Keap1 and contribute to the NQO1 inducing properties.

Detailed LC-MS and LC-$MS^2$ analyses of the GSH conjugate with the monooxygenated ligustilide species (Figure 5) revealed that at least 2 different GSH conjugates were generated (data not shown). $MS^2$ experiments provided characteristic fragment ions of the GSH moiety and the cleavage of water from the molecular ion ($MH^+$ - 18) indicated the occurrence of an additional hydroxyl group in the ligustilide species. Moreover, the UV spectra demonstrated the change of the chromophore in comparison to ligustilide (UV: $\lambda_{max}$ of ligustilide: 270, 322 nm; $\lambda_{max}$ of the GSH conjugate with the monooxygenated ligustilide species: 270 nm). Due to the reactivity of the α,β,γ,δ -unsaturated lactone and the epoxide moiety, four different GSH conjugates (SG2-SG5, Figure 5) were proposed with the intermediates, *Z*-6,7-epoxyligustilide or 3,8-epoxyligustilide. Interestingly, after application of a p.o. dose of ligustilide (500 mg/kg) to rats, a GSH conjugate with monooxygenated ligustilide (mass 206) could be detected in the plasma of these animals (72). The proposed structures represented *Z*-6,7-epoxyligustilide-SG3 and *Z*-6,7-epoxyligustilide-SG4 (Figure 5). While NMR experiments of isolated GSH conjugates would be necessary to determine the exact molecular structure, these experiments were not feasible due to the instability of not only ligustilide but also the GSH conjugates. At this point, the activity cannot be attributed to a single oxidized ligustilide or ligustilide itself, but rather to a group of non-aromatic phthalides, such as ligustilide, that are capable of cysteine alkylation.

Incubation of the *A. sinensis* partition or ligustilide with Keap1 resulted in a mass increase (Figure 4). Keap1 is a cysteine rich protein with 27 cysteine groups for human Keap1, nine of which are flanked by basic amino acid residues which increases their reactivity (19). Recent research indicates that these cysteines act as sensors for inducers (22,23). Controversy exists over which cysteine residues are the most reactive and show the strongest ARE inducing effect after alkylation (70,73-75). Known potent NQO1 inducers, including sulforaphane and the ARE inducer biotinylated iodoacetamide (BIA) have been shown to preferentially bind to three cysteines in human Keap1; Cys151, Cys288, and Cys297 (69,75). Hong et al. also detected other sulforaphane reactive cysteines including Cys196 and Cys241 (73,74). Similar experiments with ligustilide and Keap1 showed that ligustilide only alkylated Cys151, whereas oxidized ligustilide alkylated Cys151 and three other cysteines including Cys273, Cys288, and Cys319 (Table 3). The distinct pattern of modification by these two ligustilide species could be due to the relative amount of compounds in the mixture or due to differences in reactivity. Cys151 is supposed to have a key role in sensing electrophilic ARE inducers, as known inducers are reported to transmit their inducing activity through alkylating Cys151 (31,69). In support of this, Cys151S Keap1 mutants, showed lack of responsiveness to ARE inducers suggesting an important sensing role for Cys151 (23,69). Apart from Cys151, alkylation of Cys273 and Cys288 is suggested to lead to stabilization of Nrf2 and thus to a higher concentration of Nrf2 in the nucleus (69). In addition, Cys319 in human Keap1 is alkylated by oxidized ligustilide, and alkylation of this cysteine was also frequently observed by other natural ARE inducers, although its role in Nrf2 repression is not clear (31).

In conclusion, these experiments demonstrate for the first time that ligustilide and also its monooxygenated product, possibly corresponding to ligustilide epoxide, alkylate important cysteine residues in Keap1, which can lead to the accumulation of Nrf2 in the nucleus, where it enhances the transcription of ARE dependent detoxification genes. These results correlate with the potent NQO1 and ARE inducer activity of ligustilide and the *A. sinensis* partition suggesting that *A. sinensis*' dietary supplements standardized to ligustilide have the potential to help prevent cancer and other chronic diseases associated with oxidative stress. Because *A. sinensis* is frequently used for the alleviation of menopausal symptoms, this dietary supplement might have additional chemoprevention health benefits.

## Acknowledgments

The authors thank Dr. J. P. Whitlock, Jr. (Stanford University, Stanford, CA) for providing the Hepa1c1c7 cells and Drs. T.A.N. Kong, C. Chen (Rutgers University, Piscataway, NJ) and W.E. Fahl (University of Wisconsin-Madison, Madison, WI) for kindly supplying the HepG2-ARE-C8 cells. We are also grateful to Drs. A.L. Eggler, A.D. Mesecar, and. D. Lankin (UIC, Chicago, IL) for kindly providing the Keap1 protein and helpful discussions, respectively and to the Chicago Biomedical Consortium for access to the LTQ-FT ICR mass spectrometer, which was purchased with a grant from The Searle Funds at The Chicago Community Trust. This study was funded by NIH Grant P50 AT00155, jointly provided to the UIC/NIH Center for Botanical Dietary Supplements Research by the Office of Dietary Supplements and the National Center for Complementary and Alternative Medicine. Its contents are solely the responsibility of the authors and do not necessarily represent the official views of the National Center for Complementary and Alternative Medicine, the Office of Dietary Supplements, or the National Institutes of Health.

## Abbreviations

ARE, antioxidant response element
BF, 4’-bromoflavone
CD, concentration required to double the specific activity of NQO1
CI, chemopreventive index
CID, collision-induced dissociation
DPPH, 1,1-diphenyl-2-picrylhydrazyl
FAD, flavin adenine dinucleotide
GST, glutathione S-transferase
LC-MS-MS, liquid chromatography-tandem mass spectrometry
MTT, 3-(4,5-dimethylthiazo-2-yl)-2,5-diphenyltetrazolium bromide
NADP, nicotinamide adenine dinucleotide phosphate
NQO1, NAD(P)H: quinone oxidoreductase 1
ROS, reactive oxygen species
MALDI-TOF, matrix-assisted laser desorption/ionization time-of-flight
ROS, reactive oxygen species
FT-ICR, Fourier-transform ion cyclotron resonance

## References

1. Deng S, Chen SN, Yao P, Nikolic D, van Breemen RB, Bolton JL, Fong HH, Farnsworth NR, Pauli GF. Serotonergic activity-guided phytochemical investigation of the roots of Angelica sinensis. J. Nat. Prod 2006;69:536–541. [PubMed: 16643021]
2. Pharmacopoeia of the People's Republic of China. Radix Angelica sinensis. 1. Chemical Industry, Beijing, People's Republic of China; 2000.
3. Upton, R. Dang Gui (Angelica sinensis). In: Coates, P. M. e. a., editor. Encyclopedia of Dietary Supplements. Marcel Dekker; New York: 2005. p. 159-166.
4. Hou YZ, Zhao GR, Yang J, Yuan YJ, Zhu GG, Hiltunen R. Protective effect of Ligusticum chuanxiong and Angelica sinensis on endothelial cell damage induced by hydrogen peroxide. Life Sci 2004;75:1775–1786. [PubMed: 15268976]
5. Hou YZ, Zhao GR, Yuan YJ, Zhu GG, Hiltunen R. Inhibition of rat vascular smooth muscle cell proliferation by extract of Ligusticum chuanxiong and Angelica sinensis. J. Ethnopharmacol 2005;100:140–144. [PubMed: 15964163]
6. Kuang X, Yao Y, Du JR, Liu YX, Wang CY, Qian ZM. Neuroprotective role of Z-ligustilide against forebrain ischemic injury in ICR mice. Brain Res 2006;1102:145–153. [PubMed: 16806112]
7. Piersen CE. Phytoestrogens in botanical dietary supplements: implications for cancer. Integr. Cancer Ther 2003;2:120–138. [PubMed: 15035899]
8. Haranaka K, Satomi N, Sakurai A, Haranaka R, Okada N, Kosoto H, Kobayashi M. Antitumor activities and tumor necrosis factor producibility of traditional Chinese medicines and crude drugs. J. Tradit. Chin. Med 1985;5:271–278. [PubMed: 3834242]

9. Tsai NM, Lin SZ, Lee CC, Chen SP, Su HC, Chang WL, Harn HJ. The antitumor effects of Angelica sinensis on malignant brain tumors in vitro and in vivo. Clin. Cancer Res 2005;11:3475–3484. [PubMed: 15867250]
10. Tsai NM, Chen YL, Lee CC, Lin PC, Cheng YL, Chang WL, Lin SZ, Harn HJ. The natural compound n-butylidenephthalide derived from Angelica sinensis inhibits malignant brain tumor growth in vitro and in vivo. J. Neurochem 2006;99:1251–1262. [PubMed: 16987298]
11. Lee WH, Jin JS, Tsai WC, Chen YT, Chang WL, Yao CW, Sheu LF, Chen A. Biological inhibitory effects of the Chinese herb danggui on brain astrocytoma. Pathobiology 2006;73:141–148. [PubMed: 17085958]
12. Cheng YL, Chang WL, Lee SC, Liu YG, Chen CJ, Lin SZ, Tsai NM, Yu DS, Yen CY, Harn HJ. Acetone extract of Angelica sinensis inhibits proliferation of human cancer cells via inducing cell cycle arrest and apoptosis. Life Sci 2004;75:1579–1594. [PubMed: 15261763]
13. Yu Y, Du JR, Wang CY, Qian ZM. Protection against hydrogen peroxide-induced injury by Z-ligustilide in PC12 cells. Exp. Brain Res. 2007
14. Chiu PY, Leung HY, Siu AH, Poon MK, Dong TT, Tsim KW, Ko KM. Dang-Gui Buxue Tang protects against oxidant injury by enhancing cellular glutathione in H9c2 cells: role of glutathione synthesis and regeneration. Planta Med 2007;73:134–141. [PubMed: 17325989]
15. Shen G, Jeong WS, Hu R, Kong AN. Regulation of Nrf2, NF-kappaB, and AP-1 signaling pathways by chemopreventive agents. Antioxid. Redox Signal 2005;7:1648–1663. [PubMed: 16356127]
16. Chen C, Tony Kong AN. Dietary Chemopreventive compounds and ARE/EpRE Signaling. Free Radic. Biol. Med 2004;36:1505–1516. [PubMed: 15182853]
17. Hong WK, Sporn MB. Recent advances in chemoprevention of cancer. Science 1997;278:1073–1077. [PubMed: 9353183]
18. Kensler TW. Chemoprevention by inducers of carcinogen detoxication enzymes. Environ. Health Perspect 1997;105(Suppl 4):965–970. [PubMed: 9255588]
19. Dinkova-Kostova AT, Holtzclaw WD, Kensler TW. The role of Keap1 in cellular protective responses. Chem. Res. Toxicol 2005;18:1779–1791. [PubMed: 16359168]
20. Itoh K, Wakabayashi N, Katoh Y, Ishii T, Igarashi K, Engel JD, Yamamoto M. Keap1 represses nuclear activation of antioxidant responsive elements by Nrf2 through binding to the amino-terminal Neh2 domain. Genes Dev 1999;13:76–86. [PubMed: 9887101]
21. Ishii T, Itho K, Takahashi S, Sato H, Yanagawa T, Katoh Y, Bannai S, Yamamoto M. Transcription factor Nrf2 coordinately regulates a group of oxidative stress-inducible genes in macrophages. J. Biol. Chem 2000;275:16023–16029. [PubMed: 10821856]
22. Dinkova-Kostova AT, Fahey JW, Talalay P. Chemical Structures of Inducers of Nicotinamide Quinone Reductase 1 (NQO1). Meth. Enzymol 2004;382:423–448. [PubMed: 15047115]
23. Dinkova-Kostova AT, Holtzclaw WD, Cole RN, Itho K, Wakabayashi N, Katoh Y, Yamamoto M, Talalay P. Direct evidence that sulfhydryl groups of Keap1 are the sensors regulating induction of phase 2 enzymes that protect against carcinogens and oxidants. Proc. Natl. Acad. Sci. U.S.A 2002;99:11908–11913. [PubMed: 12193649]
24. Dinkova-Kostova AT, Fahey JW, Wade KL, Jenkins SN, Shapiro TA, Fuchs EJ, Kerns ML, Talalay P. Induction of the phase 2 response in mouse and human skin by sulforaphane-containing broccoli sprout extracts. Cancer Epidemiol. Biomarkers Prev 2007;16:847–851. [PubMed: 17416783]
25. Dinkova-Kostova AT, Jenkins SN, Fahey JW, Ye L, Wehage SL, Liby KT, Stephenson KK, Wade KL, Talalay P. Protection against UV-light-induced skin carcinogenesis in SKH-1 high-risk mice by sulforaphane-containing broccoli sprout extracts. Cancer Lett 2006;240:243–252. [PubMed: 16271437]
26. Zhang Y, Kensler TW, Cho CG, Posner GH, Talalay P. Anticarcinogenic activities of sulforaphane and structurally related synthetic norbornyl isothiocyanates. Proc. Natl. Acad. Sci. U.S.A 1994;91:3147–3150. [PubMed: 8159717]
27. Zhao X, Sun G, Zhang J, Strong R, Dash PK, Kan YW, Grotta JC, Aronowski J. Transcription factor Nrf2 protects the brain from damage produced by intracerebral hemorrhage. Stroke 2007;38:3280–3286. [PubMed: 17962605]

28. Kwak MK, Cho JM, Huang B, Shin S, Kensler TW. Role of increased expression of the proteasome in the protective effects of sulforaphane against hydrogen peroxide-mediated cytotoxicity in murine neuroblastoma cells. Free Radic. Biol. Med 2007;43:809–817. [PubMed: 17664144]
29. Song LL, Kosmeder JW 2nd, Lee SK, Gerhäuser C, Lantvit D, Moon RC, Moriarty RM, Pezzuto JM. Cancer chemopreventive activity mediated by 4'-bromoflavone, a potent inducer of phase II detoxification enzymes. Cancer Res 1999;59:578–585. [PubMed: 9973203]
30. Miranda CL, Aponso GL, Stevens JF, Deinzer ML, Buhler DR. Prenylated chalcones and flavanones as inducers of quinone reductase in mouse Hepa 1c1c7 cells. Cancer Lett 2000;149:21–29. [PubMed: 10737704]
31. Luo Y, Eggler AL, Liu D, Liu G, Mesecar AD, van Breemen RB. Sites of Alkylation of Human Keap1 by Natural Chemoprevention Agents. J. Am. Soc. Mass Spectrom. 2007
32. Dietz BM, Kang YH, Liu G, Eggler AL, Yao P, Chadwick LR, Pauli GF, Farnsworth NR, Mesecar AD, van Breemen RB, Bolton JL. Xanthohumol isolated from *Humulus lupulus* Inhibits menadione-induced DNA damage through induction of quinone reductase. Chem. Res. Toxicol 2005;18:1296–1305. [PubMed: 16097803]
33. Beck JJ, Chou SC. The structural diversity of phthalides from the Apiaceae. J. Nat. Prod 2007;70:891–900. [PubMed: 17477571]
34. Lin L-Z, He X-G, Lian L-Z, King W, Elliott J. Liquid chromatographicelectrospray mass spectrometric study of the phthalides of Angelica sinensis and chemical changes of Z-ligustilide. J. Chromatogr. A 1998;810:71–79.
35. Sheu SJ, Ho YS, Chen YP, Hsu HY. Analysis and processing of Chinese herbal drugs; VI. The study of Angelicae radix. Planta Med 1987;53:377–378. [PubMed: 3671555]
36. Lu GH, Chan K, Chan CL, Leung K, Jiang ZH, Zhao ZZ. Quantification of ligustilides in the roots of Angelica sinensis and related umbelliferous medicinal plants by high-performance liquid chromatography and liquid chromatography-mass spectrometry. J. Chromatogr. A 2004;1046:101–107. [PubMed: 15387176]
37. Beck JJ, Stermitz FR. Addition of methyl thioglycolate and benzylamine to (Z)-ligustilide, a bioactive unsaturated lactone constituent of several herbal medicines. An improved synthesis of (Z)-ligustilide. J Nat Prod 1995;58:1047–1055. [PubMed: 7561898]
38. Schinkovitz A, Pro S, Main M, Chen SN, Jaki BU, Lankin DC, Pauli GF. The Dynamic Nature of the Ligustilide Complex. J. Nat. Prod 2008;71:1604–1611. [PubMed: 18781813]
39. Lee SK, Mbwambo ZH, Chung H, Luyengi L, Gamez EJ, Mehta RG, Kinghorn AD, Pezzuto JM. Evaluation of the antioxidant potential of natural products. Comb. Chem. High Throughput Screen 1998;1:35–46. [PubMed: 10499128]
40. Prochaska HJ, Santamaria AB. Direct measurement of NAD(P)H:quinone reductase from cells cultured in microtiter wells: a screening assay for anticarcinogenic enzyme inducers. Anal. Biochem 1988;169:328–336. [PubMed: 3382006]
41. Fahey JW, Dinkova-Kostova AT, Stephenson KK, Talalay P. The “Prochaska” microtiter plate bioassay for inducers of NQO1. Methods Enzymol 2004;382:243–258. [PubMed: 15047106]
42. Chen C, Pung D, Leong V, Hebbar V, Shen G, Nair S, Li W, Tony Kong AN. Induction of detoxifying enzymes by garlic organosulfur compounds through transcription factor Nrf2: effect of chemical structure and stress signals. Free Radic. Biol. Med 2004;37:1578–1590. [PubMed: 15477009]
43. Liu G, Eggler AL, Dietz BM, Mesecar AD, Bolton JL, Pezzuto JM, van Breemen RB. Screening method for the discovery of potential cancer chemoprevention agents based on mass spectrometric detection of alkylated Keap1. Anal. Chem 2005;77:6407–6414. [PubMed: 16194107]
44. Frei B, Higdon JV. Antioxidant activity of tea polyphenols in vivo: evidence from animal studies. J. Nutr 2003;133:3275S–3284S. [PubMed: 14519826]
45. Ross D, Kepa JK, Winski SL, Beall HD, Anwar A, Siegel D. NAD(P)H:quinone oxidoreductase 1 (NQO1): chemoprotection, bioactivation, gene regulation and genetic polymorphisms. Chem. Biol. Interact 2000;129:77–97. [PubMed: 11154736]
46. Kang YH, Pezzuto JM. Induction of quinone reductase as a primary screen for natural product anticarcinogens. Meth. Enzymol 2004;382:380–414. [PubMed: 15047113]

47. Misico RI, Song LL, Veleiro AS, Cirigliano AM, Tettamanzi MC, Burton G, Bonetto GM, Nicotra VE, Silva GL, Gil RR, Oberti JC, Kinghorn AD, Pezzuto JM. Induction of quinone reductase by withanolides. J. Nat. Prod 2002;65:677–680. [PubMed: 12027740]
48. Quiroz-Garcia B, Figueroa R, Cogordan A, Delgado G. Photocyclodimers from Z-ligustilide. Experimental results and FMO analysis. Tetrahedron Lett 2005;46:3003–3006.
49. Chen C, Yu R, Owuor ED, Tony Kong AN. Activation of antioxidant-response element (ARE), mitogen-activated protein kinases (MAPKs) and caspases by major green tea polyphenol components during cell survival and death. Arch. Pharm. Res 2000;23:605–612. [PubMed: 11156183]
50. Dieckhaus CM, Fernandez-Metzler CL, King R, Krolikowski PH, Baillie TA. Negative ion tandem mass spectrometry for the detection of glutathione conjugates. Chem. Res. Toxicol 2005;18:630–638. [PubMed: 15833023]
51. Yi T, Leung KS, Lu GH, Zhang H. Comparative analysis of Ligusticum chuanxiong and related umbelliferous medicinal plants by high performance liquid chromatography-electrospray ionization mass spectrometry. Planta Med 2007;73:392–398. [PubMed: 17372865]
52. Ozaki Y, Sekita S, Harada M. [Centrally acting muscle relaxant effect of phthalides (ligustilide, cnidilide and senkyunolide) obtained from Cnidium officinale Makino]. Yakugaku Zasshi 1989;109:402–406. [PubMed: 2810059]
53. Matsumoto K, Kohno S, Ojima K, Tezuka Y, Kadota S, Watanabe H. Effects of methylenechloride-soluble fraction of Japanese angelica root extract, ligustilide and butylidenephthalide, on pentobarbital sleep in group-housed and socially isolated mice. Life Sci 1998;62:2073–2082. [PubMed: 9627086]
54. Hlubik P, Stritecka H. Antioxidants--clinical aspects. Cent. Eur. J. Public Health 2004;12 (Suppl):S28–30. [PubMed: 15141970]
55. Wu SJ, Ng LT, Lin CC. Antioxidant activities of some common ingredients of traditional chinese medicine, Angelica sinensis, Lycium barbarum and Poria cocos. Phytother. Res 2004;18:1008–1012. [PubMed: 15742346]
56. Li SY, Yu Y, Li SP. Identification of antioxidants in essential oil of radix Angelicae sinensis using HPLC coupled with DAD-MS and ABTS-based assay. J. Agric. Food Chem 2007;55:3358–3362. [PubMed: 17411069]
57. Saito ST, Gosmann G, Saffi J, Presser M, Richter MF, Bergold AM. Characterization of the constituents and antioxidant activity of Brazilian green tea (Camellia sinensis var. assamica IAC-259 cultivar) extracts. J. Agric. Food Chem 2007;55:9409–9414. [PubMed: 17937477]
58. Jaiswal AK. Characterization and partial purification of microsomal NAD(P)H:quinone oxidoreductases. Arch. Biochem. Biophys 2000;375:62–68. [PubMed: 10683249]
59. Joseph P, Long DJ 2nd, Klein-Szanto AJ, Jaiswal AK. Role of NAD(P)H:quinone oxidoreductase 1 (DT diaphorase) in protection against quinone toxicity. Biochem. Pharmacol 2000;60:207–214. [PubMed: 10825465]
60. Bolton JL, Yu L, Thatcher GR. Quinoids formed from estrogens and antiestrogens. Meth. Enzymol 2004;378:110–123. [PubMed: 15038960]
61. Bolton JL. Quinoids, quinoid radicals, and phenoxyl radicals formed from estrogens and antiestrogens. Toxicology 2002;177:55–65. [PubMed: 12126795]
62. Zhu H, Jia Z, Mahaney JE, Ross D, Misra HP, Trush MA, Li Y. The highly expressed and inducible endogenous NAD(P)H:quinone oxidoreductase 1 in cardiovascular cells acts as a potential superoxide scavenger. Cardiovasc. Toxicol 2007;7:202–211. [PubMed: 17901563]
63. Chen XL, Varner SE, Rao AS, Grey JY, Thomas S, Cook CK, Wasserman MA, Medford RM, Jaiswal AK, Kunsch C. Laminar flow induction of antioxidant response element-mediated genes in endothelial cells. A novel anti-inflammatory mechanism. J. Biol. Chem 2003;278:703–711. [PubMed: 12370194]
64. Fourie J, Guziec F Jr. Guziec L, Monterrosa C, Fiterman DJ, Begleiter A. Structure-activity study with bioreductive benzoquinone alkylating agents: effects on DT-diaphorase-mediated DNA crosslink and strand break formation in relation to mechanisms of cytotoxicity. Cancer Chemother. Pharmacol 2004;53:191–203. [PubMed: 14614574]

65. Ross D, Beall H, Traver RD, Siegel D, Phillips RM, Gibson NW. Bioactivation of quinones by DT-diaphorase, molecular, biochemical, and chemical studies. Oncol. Res 1994;6:493–500. [PubMed: 7620217]
66. Dinkova-Kostova AT, Massiah MA, Bozak RE, Hicks RJ, Talalay P. Potency of Michael reaction acceptors as inducers of enzymes that protect against carcinogenesis depends on their reactivity with sulfhydryl groups. Proc. Natl. Acad. Sci. U.S.A 2001;98:3404–3409. [PubMed: 11248091]
67. Dinkova-Kostova AT, Talalay P. Relation of structure of curcumin analogs to their potencies as inducers of Phase 2 detoxification enzymes. Carcinogenesis 1999;20:911–914. [PubMed: 10334211]
68. Xiao H, Parkin K. Isolation and identification of phase II enzyme-inducing agents from nonpolar extracts of green onion (Allium spp.). J. Agric. Food Chem 2006;54:8417–8424. [PubMed: 17061815]
69. Zhang DD, Hannink M. Distinct cysteine residues in Keap1 are required for Keap1-dependent ubiquitination of Nrf2 and for stabilization of Nrf2 by chemopreventive agents and oxidative stress. Mol. Cell. Biol 2003;23:8137–8151. [PubMed: 14585973]
70. Eggler AL, Liu G, Pezzuto JM, van Breeman RB, Mesecar AD. Modifying specific cysteines of the electrophile-sensing human Keap1 protein is insufficient to disrupt binding to the Nrf2 domain Neh2. Proc. Natl. Acad. Sci. U.S.A 2005;102:10070–10075. [PubMed: 16006525]
71. Deng S, Chen SN, Lu J, Wang ZJ, Nikolic D, van Breemen RB, Santarsiero BD, Mesecar A, Fong HH, Farnsworth NR, Pauli GF. GABAergic phthalide dimers from Angelica sinensis (Oliv.) Diels. Phytochem. Anal 2006;17:398–405. [PubMed: 17144247]
72. Yan R, Ko NL, Li SL, Tam YK, Lin G. Pharmacokinetics and metabolism of ligustilide, a major bioactive component in Rhizoma Chuanxiong, in the rat. Drug Metab. Dispos 2008;36:400–408. [PubMed: 18039808]
73. Hong F, Freeman ML, Liebler DC. Identification of sensor cysteines in human Keap1 modified by the cancer chemopreventive agent sulforaphane. Chem. Res. Toxicol 2005;18:1917–1926. [PubMed: 16359182]
74. Hong F, Sekhar KR, Freeman ML, Liebler DC. Specific patterns of electrophile adduction trigger Keap1 ubiquitination and Nrf2 activation. J. Biol. Chem 2005;280:31768–31775. [PubMed: 15985429]
75. Eggler AL, Luo Y, van Breemen RB, Mesecar AD. Identification of the Highly Reactive Cysteine 151 in the Chemopreventive Agent-Sensor Keap1 Protein is Method-Dependent. Chem. Res. Toxicol. 2007
76. Yoshiki Y, Kahara T, Okubo K, Sakabe T, Yamasaki T. Superoxide- and 1,1-diphenyl-2-picrylhydrazyl radical-scavenging activities of soyasaponin beta g related to gallic acid. Biosci. Biotechnol. Biochem 2001;65:2162–2165. [PubMed: 11758904]
77. Gerhäuser C, Alt A, Heiss E, Gamal-Eldeen A, Klimo K, Knauft J, Neumann I, Scherf HR, Frank N, Bartsch H, Becker H. Cancer chemopreventive activity of xanthohumol, a natural product derived from hop. Mol. Cancer Ther 2002;1:959–969. [PubMed: 12481418]
78. Yu R, Mandlekar S, Lei W, Fahl WE, Tan TH, Tony Kong AN. p38 mitogen-activated protein kinase negatively regulates the induction of phase II drug-metabolizing enzymes that detoxify carcinogens. J. Biol. Chem 2000;275:2322–2327. [PubMed: 10644681]
79. Kaouadji M, De Pachtere F, Pouget C, Chulia A. Three additional phthalide derivatives, an epoxymonomer and two dimers, from Ligusticum wallichii Rhizomes. J. Nat. Prod 1986;49:872–877.
80. Keum YS, Owuor ED, Kim BR, Hu R, Kong AN. Involvement of Nrf2 and JNK1 in the activation of antioxidant responsive element (ARE) by chemopreventive agent phenethyl isothiocyanate (PEITC). Pharm. Res 2003;20:1351–1356. [PubMed: 14567627]
81. Bloom DA, Jaiswal AK. Phosphorylation of Nrf2 at Ser40 by protein kinase C in response to antioxidants leads to the release of Nrf2 from INrf2, but is not required for Nrf2 stabilization/accumulation in the nucleus and transcriptional activation of antioxidant response element-mediated NAD(P)H:quinone oxidoreductase-1 gene expression. J. Biol. Chem 2003;278:44675–44682. [PubMed: 12947090]

82. Lee JM, Moehlenkamp JD, Hanson JM, Johnson JA. Nrf2-dependent activation of the antioxidant responsive element by tert-butylhydroquinone is independent of oxidative stress in IMR-32 human neuroblastoma cells. Biochem. Biophys. Res. Commun 2001;280:286–292. [PubMed: 11162512]

83. Lee JM, Anderson PC, Padgitt JK, Hanson JM, Waters CM, Johnson JA. Nrf2, not the estrogen receptor, mediates catechol estrogen-induced activation of the antioxidant responsive element. Biochim. Biophys. Acta 2003;1629:92–101. [PubMed: 14522084]

84. Hayes JD, McMahon M. Molecular basis for the contribution of the antioxidant responsive element to cancer chemoprevention. Cancer Lett 2001;174:103–113. [PubMed: 11689285]

85. Itoh K, Chiba T, Takahashi S, Ishii T, Igarashi K, Katoh Y, Oyake T, Hayashi N, Satoh K, Hatayama I, Yamamoto M, Nabeshima Y. An Nrf2/small Maf heterodimer mediates the induction of phase II detoxifying enzyme genes through antioxidant response elements. Biochem. Biophys. Res. Commun 1997;236:313–322. [PubMed: 9240432]

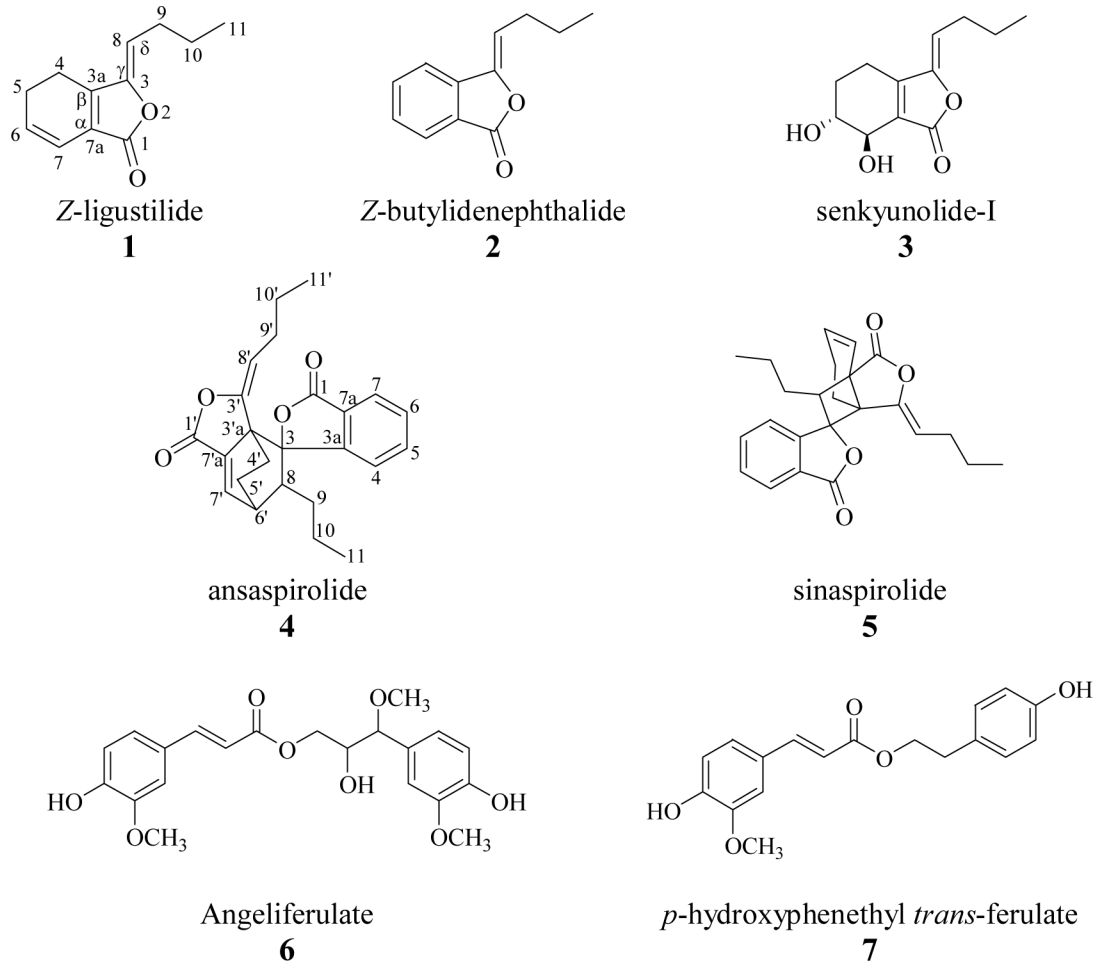


**Figure 1.**
Chemical structures of isolated compounds from *Angelica sinensis* (1).

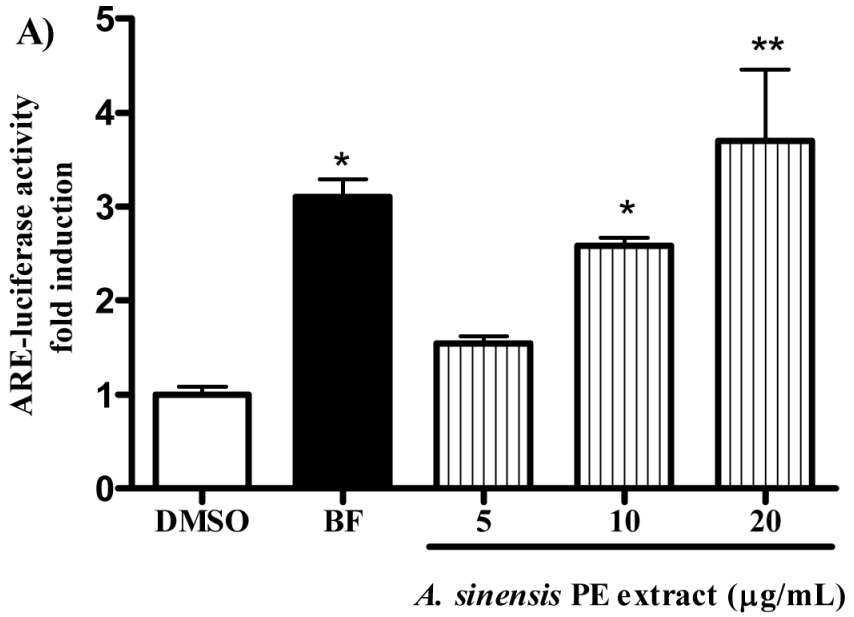


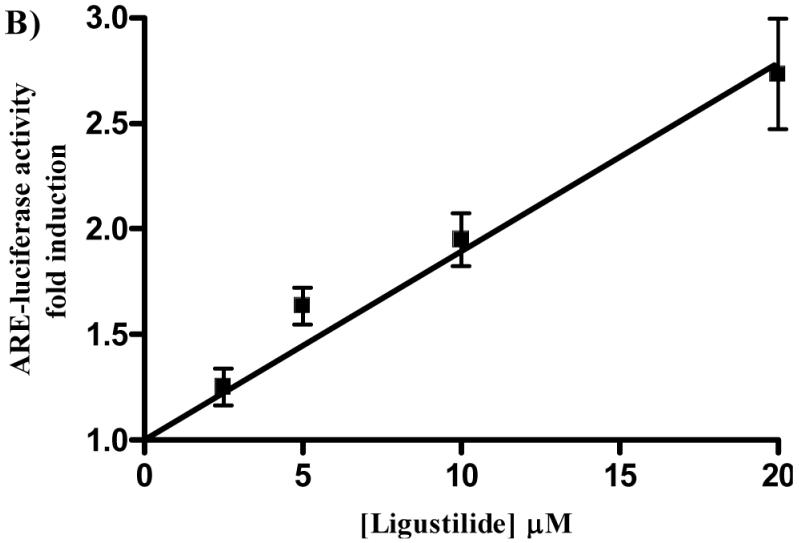


**Figure 2.**

Induction of ARE-luciferase reporter activity by A) *Angelica sinensis* and B) ligustilide. Stably transfected HepG2-ARE-C8 cells (78) were plated in 6-well plates at a density of $1 \times 10^5$ cells/mL and incubated overnight. Cells were stimulated with different concentrations of extract, ligustilide, BF as a positive control (664 nM), or DMSO as a negative control. Cells were harvested 18 h after treatment. Luciferase activity was determined and normalized by protein determination. The data were obtained from three separate experiments and expressed as fold induction compared to the control (DMSO-treated cells) ± SD.

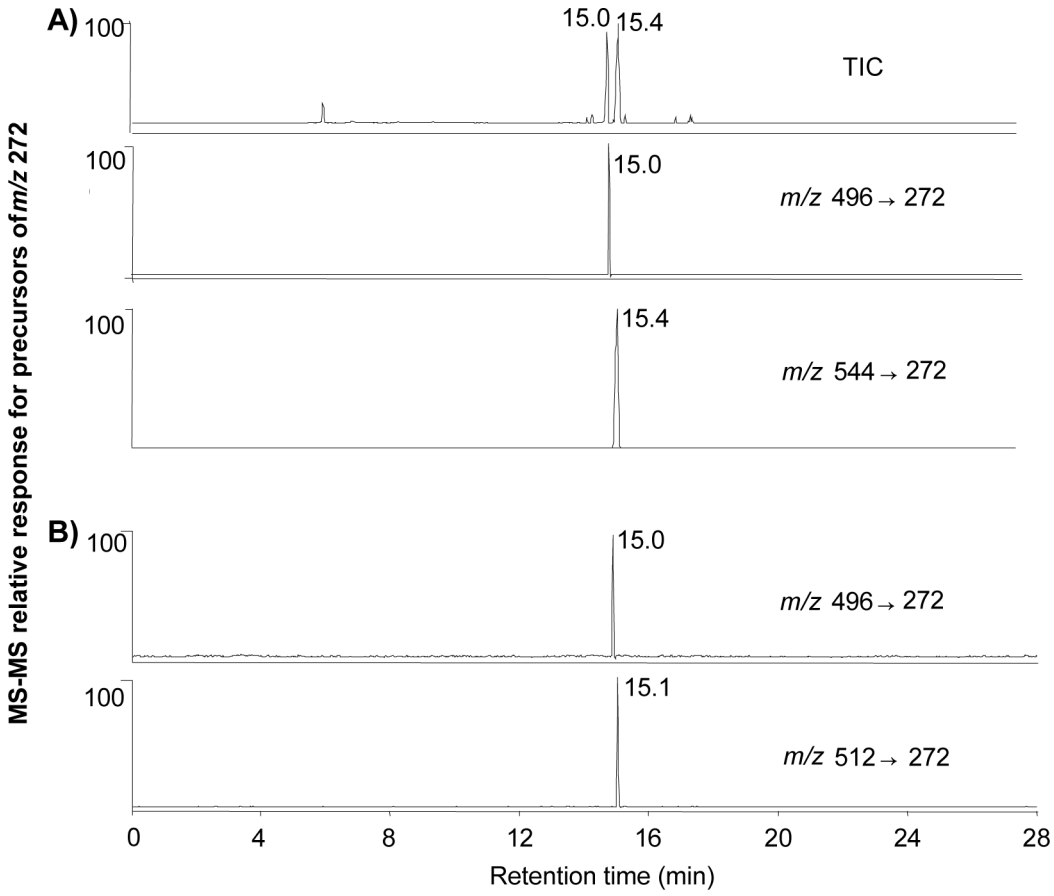


**Figure 3.**

Negative ion electrospray LC-MS-MS chromatograms of the petroleum ether partition of *A. sinensis* or the isolated *A. sinensis* constituent *Z*-ligustilide after incubation with GSH in 25 mM Tris-HCl buffer (pH 8.0) for 1 h at room temperature (50). A) *Angelica sinensis* partition after incubation with GSH. The negative ion LC-MS-MS precursor ion scan of *m/z* 272 identified two major GSH conjugates eluting at 15.0 and 15.4 min with *m/z* values of 496 and 544, respectively. B) Ligustilide after incubation with GSH (molar ratio of 1:10, ligustilide/GSH). The negative ion LC-MS-MS precursor ion scan of *m/z* 272 identified two major GSH conjugates eluting at 15.0 and 15.1 min with *m/z* values of 496 and 512, respectively. Note that the GSH conjugates of *m/z* 496 formed during incubations with *A. sinensis* and ligustilide both eluted at 15.0 min during LC-MS.

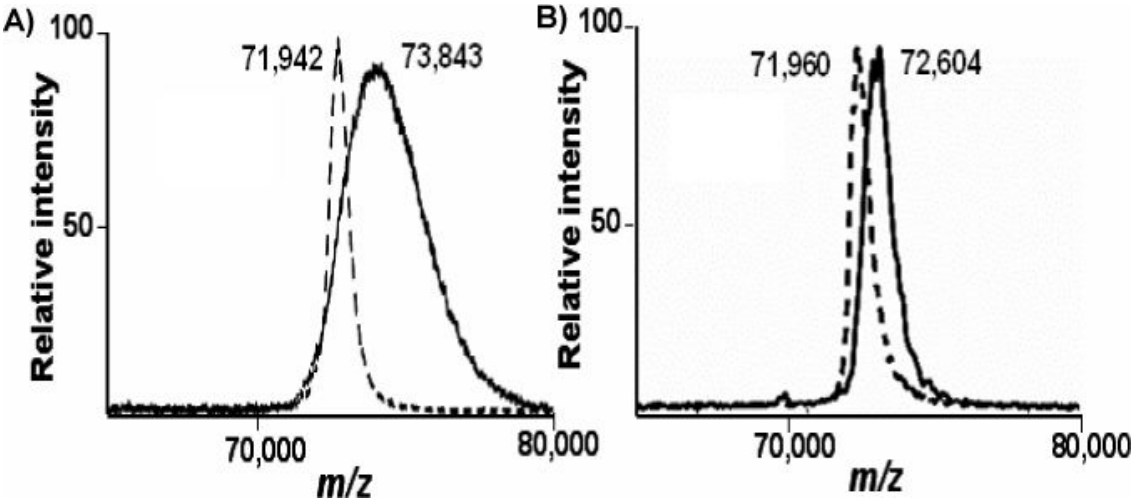


**Figure 4.**

Positive ion MALDI-TOF mass spectra of Keap1 (5 μM) following incubation for 1 h with A) *Angelica sinensis* partition (100 $\mu$g/mL); or B) ligustilide (100 $\mu$M) in 25 mM Tris-HCl buffer (pH 8.0) at room temperature (43). The dashed lines indicate Keap1 incubated with buffer as a control, and the solid lines represent Keap1 incubated with either the *A. sinensis* partition or ligustilide. The mass shifts of the Keap1 protein after the incubation indicate that both *Angelica sinensis* partition and ligustilide alkylate Keap1 protein.

**Proposed monooxidation products of *Z*-ligustilide 1:**

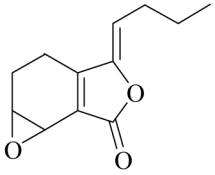


*Z*-6,7-epoxyligustilide

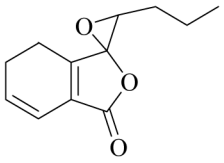


3,8-epoxyligustilide

**Proposed GSH conjugates with *Z*-ligustilide 1:**

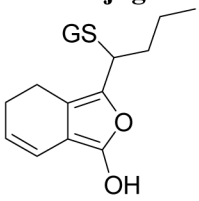


*Z*-ligustilide-SG1a

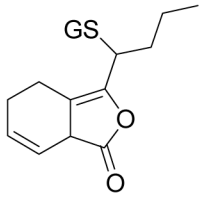


*Z*-ligustilide-SG1b

**Proposed GSH conjugates with the monooxidation product of ligustilide:**

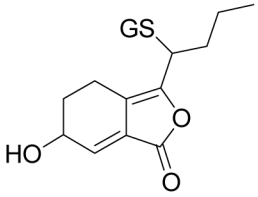


*Z*-6,7-epoxyligustilide-SG2

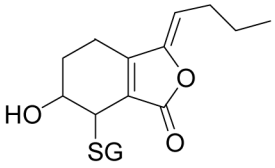


*Z*-6,7-epoxyligustilide-SG3

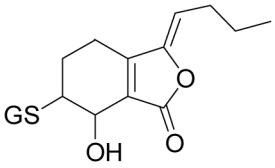


*Z*-6,7-epoxyligustilide-SG4

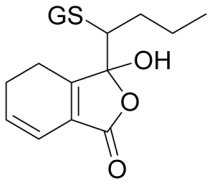


3,8-epoxyligustilide-SG5

**Figure 5.**

Proposed monooxidation products of ligustilide with the mass of 206 (34,38,79) and possible GSH-conjugates with ligustilide **1** or with its monooxidation product (72).

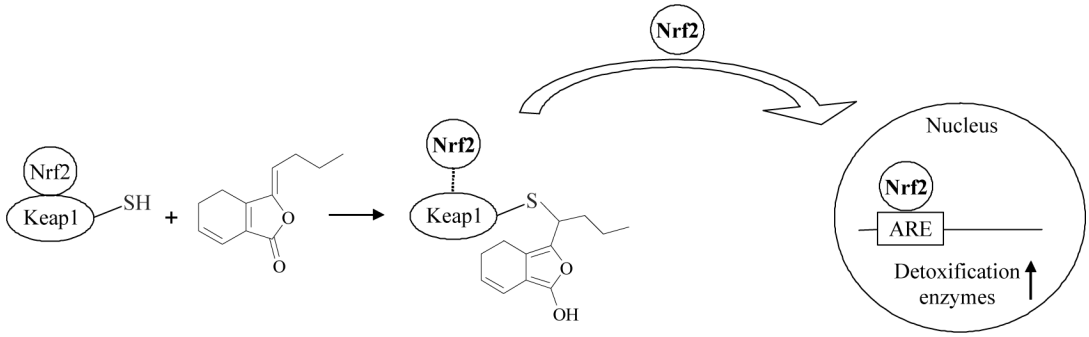


**Scheme 1.**

Proposed mechanism of NQO1 induction by ligustilide through the Keap1-Nrf2 pathway. Besides Keap1, the mitogen-activated protein kinase (MAPK) (78,80), the protein kinase C (PKC) (81) and the phosphatidylinositol 3-kinase (PI3K) pathways (82,83) play roles in the regulation of detoxification enzymes (16). PKC phosphorylation of serine-40 in Nrf2 is also involved in this pathway (81). Within the nucleus, Nrf2 binds to the ARE as a heterodimer with either small Maf proteins, FosB, c-Jun, or JunD (84,85). These proteins are omitted for clarity.

**Table 1**

Activities of a methanol *A. sinensis* extract, its partitions and isolated compounds from the petroleum ether and chloroform partitions in the DPPH-, NQO1-, and cytotoxicity-assays.

| | Extract/compounds | DPPH % FRS[a] ± SD | NQO1 assay CD[b] [μg/mL or μM] ± SD | Cytotoxicity $IC_{50}$[c] [μg/mL or μM] ± SD | CI[d] |
|---|---|---|---|---|---|
| | Methanol extract | < 50 | > 20 | > 20 | - |
| | Petroleum ether partition | < 50 | 5.5 ± 0.7 | 103.1 ± 14.1 | 19 |
| | Chloroform partition | 63 ± 1 | 3.9 ± 0.5 | 67.5 ± 3.2 | 17 |
| | Butanol partition | < 50 | > 20 | > 20 | - |
| | Water partition | < 50 | > 20 | > 20 | - |
| | **Isolated compounds** | | | | |
| **1** | *Z*-ligustilide (98%) | < 50 | 6.9 ± 1.9 | 71.2 ± 4.1 | 10 |
| | *Z*-ligustilide (58%) | NA | 7.2 ± 1.4 | > 20 | |
| **2** | *Z*-butylidenephthalide | < 50 | > 20 | > 20 | - |
| **3** | senkyunolide I | < 50 | 17.9 ± 0.6 | > 20 | - |
| **4** | ansaspirolide | < 50 | 0.9 ± 0.1 | 2.9 ± 0.1 | 3 |
| **5** | sinaspirolide | < 50 | > 20 | > 20 | - |
| **6** | angeliferulate | NA[e] | 7.5 ± 0.2 | > 20 | - |
| **7** | *p*-hydroxyphenethyl *trans*-ferulate | 65 ± 1 | 2.4 ± 0.3[f] | > 20 | - |

[a] % FRS represents the percent of free radical scavenged at a screening concentration of 100 μg/mL for extracts and 100 μM for pure compounds. Gallic acid was used as positive control ($IC_{50}$ = 34 μM). The $IC_{50}$ is consistent with literature data (76).

[b] CD value represents the concentration required for two-fold induction of NQO1. Each CD value was determined by at least two experiments performed independently with duplicate measurements. If CD > 20 μg/mL or 20 μM, it was deemed inactive. 4'-Bromoflavone (CD = 0.08 ± 0.02 μM) was used as a positive control in the NQO1 assay; its CD value was consistent with literature data (77). The purity of each isolated compound was tested by GC-MS.

[c] $IC_{50}$: The concentration of compound or extract needed to inhibit cell growth in Hepa1c1c7 by 50% using the crystal violet cytotoxicity assay.

[d] CI: Chemopreventive Index: $IC_{50}$/CD.

[e] Compound was not tested in the DPPH assay due to lack of sufficient material.

[f] Compound **7** has been isolated from green onions previously and tested for NQO1 induction (CD value = 6.6 μM (68).

**Table 2**

Theoretical and measured accurate masses for the determination of the elemental composition of the GSH conjugates.

| Ligustilide species | Molecular formula and theoretical mass of each compound before conjugation | Theoretical molecular formula and mass of each GSH conjugate $[M+H]^+$ | Observed mass of each GSH conjugate[a] $[M+H]^+$ | Mass accuracy (Δppm)[b] |
|---|---|---|---|---|
| *Z*-ligustilide | $C_{12}H_{14}O_2$ (190.0988) | $[C_{22}H_{32}N_3O_8S]^+$ (498.1905) | 498.1911 | + 1.2 |
| oxidized ligustilide species | $C_{12}H_{14}O_3$ (206.0938) | $[C_{22}H_{32}N_3O_9S]^+$ (514.1854) | 514.1860 | + 1.2 |

[a] The accurate mass was measured using positive ion electrospray with a hybrid linear ion trap FT ICR mass spectrometer.

[b] ppm: Parts per million.

**Table 3**

Cysteine residues in Keap1 protein modified by ligustilide species.

| Keap1 tryptic peptides | Cysteines | *Z*-ligustilide | Oxidized ligustilide |
|---|---|---|---|
| CVLHVMNGAVMYQIDSVVR | Cys 151 | 1,2,3[a] | 1,2,3 |
| CHSLTPNFLQMQLQK | Cys 273 | | 1,2,3 |
| CEILQSDSR | Cys 288 | | 1,2,3 |
| IFEELTLHKPTQVMPCR | Cys 319 | | 2,3 |

[a]These data represent the results of three independent LC-MS-MS analyses. Numbers indicate the experiment numbers (1, 2, and 3) in which specific modified cysteines were detected.